Title Modification of aluminum 1050 and 2219 alloys using CuBr nanosecond laser for hydrophobic and hydrophilic properties

Antons Pecejs [1, *], Emil Yankov [2, *], Imants Adijans [1], Edmunds Teirumnieks [1] and Lyubomir Lazov [1]

[1] Rezekne Academy of Technologies, Faculty of Engineering, Rezekne, Latvia 1; antons.pacejs@rta.lv; imants.adijans@rta.lv; edmunds.teirumnieks@rta.lv; lyubomir.lazov@rta.lv

[2] Uneversity of Ruse "Angel Kanchev", Materials Science and Technology, Bulgaria 2; eyankov@uni-ruse.bg

* Correspondence: antons.pacejs@rta.lv; eyankov@uni-ruse.bg

† This paper is an extended version of our paper published in Presented at the 4th International Electronic Conference on Applied Sciences, 27 Oct–10 Nov 2023; Available online: https://asec2023.sciforum.net/

Abstract: This study investigates the use of CuBr vapor nanosecond laser with 510 nm / 578.2 nm wavelength for surface treatment of 1050 aluminum and 2219 aluminum alloys. Laser-induced periodic surface structuring was used to optimize processing parameters to achieve hydrophobic and hydrophilic properties on the surface. The wetting properties were measured and the roughness results (Ra, Rz, Rq) evaluated. Prior to and after laser treatment, surface wetting and roughness changes were investigated. The wetting study showed that the maximum contact angle between a droplet of deionized water and the treated surface can be reached between more than 140 degrees and less than 10 degrees, which, respectively, is a super hydrophobic and hydrophilic surface. Compared to untreated surface, wetting increased by more than 2 times and decreased more than 8 times. Overall, experiments show the dependence of wetting properties on laser input parameters such as scan speed, scan line distance with different delivered energy amounts. This study demonstrates the possibility of laser parameter optimization which do not require auxiliary gases and additional processing of the resulting surfaces to obtain different wetting properties on the surface. The findings described in this article suggest that CuBr laser surface treatment method is a promising method for industrial applications where surfaces with special wetting and roughness properties are required, as an example of laser marking of serial number of parts used in wet environments such as aerospace, shipbuilding and defense industries.

Keywords: hydrophobic, hydrophilic, aluminum, roughness, laser texturing, CuBr laser

1. Introduction

Photon-electron interaction is a crucial technique used in surface science, materials science, and condensed matter physics. This phenomenon enables the study of surface properties at an atomic level [1]. Consequently, the material undergoes modifications in surface morphology, chemical composition, and surface properties [2]. Nanosecond lasers find use in many industrial applications, therefore picosecond and femtosecond lasers are useful in applications that require high precision and minimal damage to the surrounding material. All three types of lasers have their advantages and disadvantages and complement each other in various industrial applications [3]. Laser-based surface treatments can modify the surface structure of a material, leading to changes in its surface energy and wetting properties. Limited research has been conducted to examine the surface's long-term durability against organic contamination [4]. Currently, there is a limited amount of research on the utilization of CuBr vapor lasers for aluminum treatment. One of the studies in this area focuses on titanium ablation using CuBr laser [5], while another study in

2021 achieved a record high average laser power of 140 W through the use of an atomically self-terminating CuBr vapor laser [6]. However, there is a lack of literature on the use of CuBr vapor lasers for material treatment and investigating roughness and wetting properties, as this has not been explored in previous studies. The present study aimed to investigate the effects of Cooper bromide vapor nanosecond laser treatment on the surface morphology, roughness, and wetting properties of aluminum 1050 and aluminum 2219 alloys. In a recent report, A.O. Ijaola et al. [7] conducted a review on the surface wetting properties of different materials researches published between the years 2003 and 2022. The report provides a comprehensive and critical analysis of superhydrophobic surfaces that have been laser textured on different substrate materials. In another review article, M.M. Quazi et al. [8] authors provide a summary of the surface treatment and modification of aluminum and its alloys using laser systems such as CO2, diode laser, Nd:YAG, Yb-Fiber, Ruby, and Excimer. As well as article offers an overview of the various techniques employed in laser surface treatment of aluminum and its alloys. D.V. Zaitseva et al. [9] report on the behavior of water droplets on laser-modified surfaces of aluminum alloy (AMg6). The surfaces were modified using laser ablation with a 1064 nm Ytterbium nanosecond pulsed fiber laser. The article provides details on the experiment and the observed behavior of the water droplets on the laser-modified surfaces. M.V. Rukosuev et al. [10] conducted research on the use of femtosecond laser ablation as a potential method for producing hydrophobic micro- and nanostructures on austenitic stainless steel (AISI 316L) surfaces. The authors successfully generated hierarchical structures on the surface, which led to super-hydrophobic properties. Additionally, laser ablation of the surfaces resulted in dual-scale hierarchical structures, further enhancing the hydrophobicity to 167° contact angle (CA). The study demonstrates the potential of femtosecond laser ablation as a method for creating hydrophobic surfaces with micro- and nanostructures on AISI 316L. L. Ruiz de Lara et al. [11] conducted a study on the formation of laser-patterned ultrahydrophobic aluminum surfaces and evaluated their corrosion resistance using polarization curves and open circuit potential measurements. The article describes the process of creating these surfaces using laser patterning techniques and provides details on the testing methods used to assess their corrosion resistance. The study highlights the potential of laser patterning to create ultrahydrophobic surfaces with improved corrosion resistance properties. In another research, Rafieazad Mehran et al. [12] shows that surface hydrophobicity does not necessarily improve the corrosion resistance of a sample. The article presents a critical evaluation of the relationship between surface hydrophobicity and corrosion resistance and highlights the need for further investigation to better understand this relationship. Zhenhui Chen et al. [13] used a picosecond laser to modify the surface of a pure aluminum sheet with a wavelength of 1064 nm, a repetition rate of 1000 kHz, and a scanning speed of 0.4 m/s. The laser treatment resulted in a superhydrophilic and light absorbent surface, which the authors suggest may be suitable for enhancing the efficiency of solar desalination. The study suggests that picosecond laser-treated aluminum surfaces have significant potential for sustainable desalination applications. As such, the utilization of CuBr vapor laser to achieve similar results could be a promising area for further research. To conclude, limited research exists on the effects of dual wavelength CuBr laser treatment on materials, but it has shown potential for enhancing the wetting and roughness properties of aluminum alloys, making it useful in industries such as aerospace, automotive, and construction.

2. Materials and Methods

2.1. Laser

The surfaces of aluminum alloy sheets were irradiated with a Copper Bromide vapor laser system (Institute of Solid State Physics, Sofia, Bulgaria) operating at dual wavelength 510 nm and 578.2 nm. To conduct material treatment experiments, a range of processing parameters were employed. These parameters include a scanning speed varying from 2

mm/s to 300 mm/s, a scanning interval varying between 10 μm and 90 μm and an average power ranging from 2 W to 10 W. Additionally, the impulse width and repetition rate was set at 30 ns and 20 kHz respectively with an impulse energy of 1.2 mJ, beam quality M^2 < 1.5 and laser spot diameter of 40 μm. The principal scheme of laser treatment experiments could be observed in Figure 1.
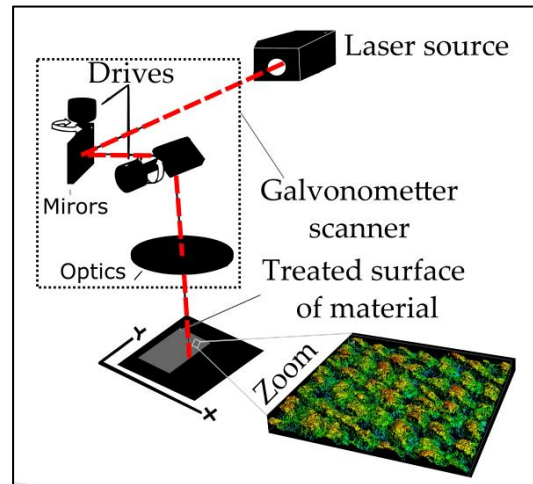
Figure 1. Schematic representation of laser treatment of samples.

The laser was focused onto the sample surface using an F-theta lens with 30 μm spot size. More specific mechanical engineering details about the laser could be found in the research paper of the owner of this specific laser system [14]. To investigate the impact of laser processing parameters on material properties, a parameter matrix was developed in which two parameters were varied while others remained constant. Therefore, for a better understanding of the impact of laser processing parameters mathematical equations can be employed to establish correlations between the processing parameters and the resulting material properties e.g. the roughness and wetting.

Average energy density ($\bar{E}$) is a parameter in laser processing, which determine the amount of average energy delivered per unit area to the material. It can be calculated by using equation (1):

$$\bar{E} = \frac{(A \times P)}{(v \times \Delta x)} \, , \tag{1}$$

where: A – coefficient of reflection for aluminum 0.7; P – average power of laser in W; v – scanning speed in mm/s; Δx – distance between scanning lines in mm. The unit of average energy density is J/mm².

Pulse overlap (K_{ov}) is parameter in laser processing, which determines the pulse overlap in percent within single laser scanning path. It can be calculated by using equation (2):

$$K_{ov} = \left(1 - \frac{v}{f \times d} \right) \times 100 \, , \tag{2}$$

where: f – repetition rate frequency in Hz, v – scanning speed in mm/s, d - diameter of focal spot of the laser in mm. The unit of pulse overlap is percents.
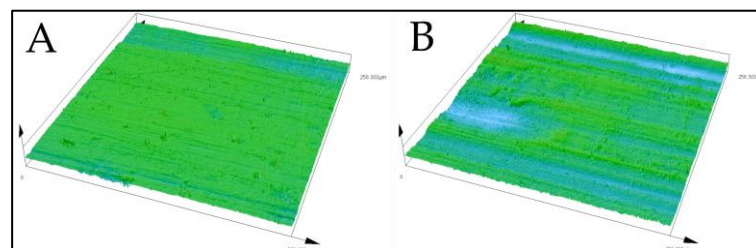
2.2. Material

For this study, aluminum 2219 and 1050 alloys sheets with dimensions 100 mm x 60 mm x 2 mm were used, see Table 1 with chemical compositions, initial surface roughness, melting point, thermal conductivity and initial surface contact angle (CA) of aluminum alloys.

During the research, the materials before the irradiance with the laser were cleaned with isopropanol, dried and kept in room conditions for 24 hours. After the laser treatment, the material samples were again cleaned with isopropanol in an ultrasound bath for 1 hour, then dried and kept in room condition for 24 hours. It should be noted that the material was not subjected to any mechanical treatment and surfaces observed in Figure 2 are made by the manufacturer.

Table 1. Chemical composition of aluminum alloy 2219 and aluminum alloy 1050.

| Alloy	Chemical Composition (%)	Melting point, (°C)	Thermal conductivity, (W/m*K)	Initial surface roughness, (µm)	Initial surface (CA, °)
Aluminum 1050	Al: 99.6 ± 0,08, Si: 0.26 ± 0.025, Fe: 0.41 ± 0.01, Cu: 0.04 ± 0.03, Mn: 0.04 ± 0.02, Mg: 0.04 ± 0.02, Zn: 0.04 ± 0.01, Ti: 0.02 ± 0.01 , Cr: 0.02 ± 0.01, Other: 0.02 ± 0.01	648 ± 3	221 ± 2	Ra = 0.156 ± 0.022 Rz = 3.97 ± 0.032 Rq = 0.201 ± 0.020	73 ± 1
Aluminum 2219	Al: 91.5 ± 0,51 Cu: 6.2 ± 0.60, Zn: 0.50 ± 0.20, Mn: 0.30 ± 0.1 0, Mg: 0.03 ± 0.07, Ti: 0.06 ± 0.04, Cr: 0.06 ± 0.04, Other: <0.10	542 ± 2	150 ± 2	Ra = 0.318 Rz = 4.19 Rq = 0.387	68 ± 1

Figure 2. Material surface before laser treatment, where: A- Al alloy 1050, B - Al alloy 2219.

2.3. Wettability

The angle of the deionized water droplet was measured using a principal diagram which is shown in Figure 3. Dosing the drop is a manual dosing micropipette. The controlled dose of the drop is 50 µm, which is administered manually. On each marking, 5

(**a**)   (**b**)
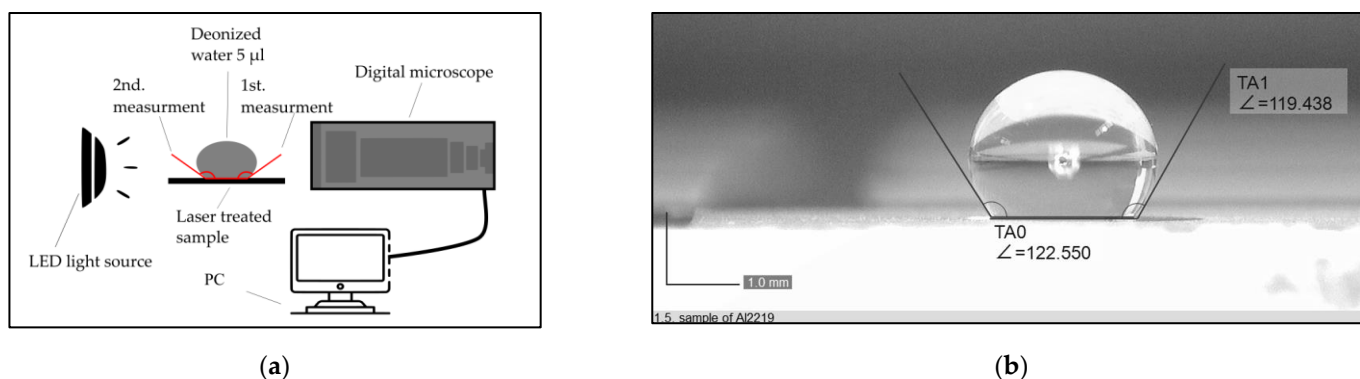
Figure 3. The wettability measurement scheme (**a**) of laser treated samples; (**b**) The view of CA measurement made in DinoLite software for single laser treated sample.
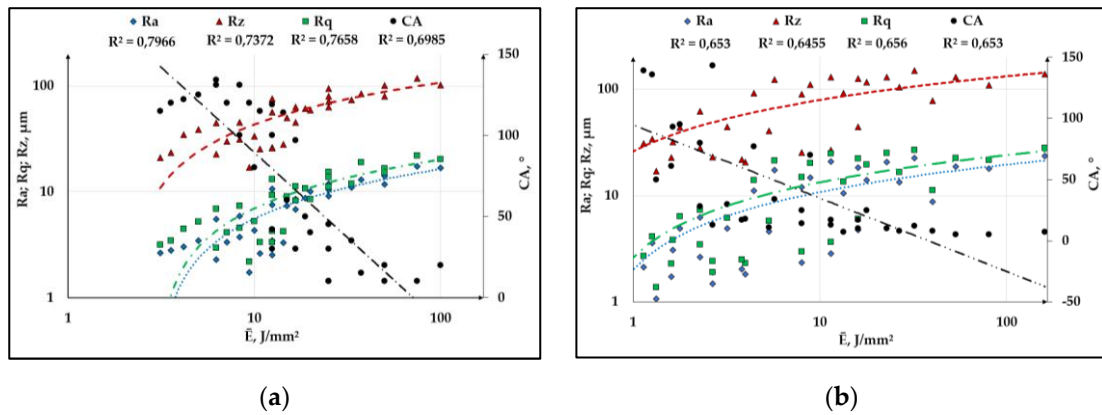
2.4. Roughness

To measure surface roughness, an Olympus OLS 5000 laser scanning microscope with an ×50 lens which ensures ×1125 magnification and a scan area of 258 μm x 258 μm was selected to conduct measurements. Should be noted, that the laser scanning microscope was utilized to scan the sample surface with pitch of scanning 0.4 μm which corresponds to "fine" measurement option in OLS software, then the resulting data was analyzed using the built-in software to generate a 3D topography map, intensity profile and true color image of the sample in magnification. The roughness parameters, R_a, R_q and R_z were calculated from the 3D topography map automatically.

3. Results and discussion

In this section, the plotted data trends for wetting, roughness and derived variable values which were obtained by treatment of materials using CuBr vapor laser with different processing parameters could be observed. Trend lines with higher R-squared coefficient, indicating a stronger correlation were chosen for all plotted data. Difference in laser applied parameters for two processed alloys appears because of the parameters' optimization, which was made to obtain hydrophobic and hydrophilic properties on different aluminum alloy materials.

Two models can describe the correlation between surface roughness and hydrophobicity in the context of surface wettability. The Wenzel model predicts an increase in the apparent contact angle for hydrophobic surfaces and a decrease for hydrophilic surfaces as surface roughness increases. However, this model cannot describe the behavior of laser textured surfaces that change the wettability of the surface from hydrophilic to hydrophobic. The Cassie-Baxter model assumes that droplets do not wet rough surfaces completely due to trapped air packs within the surface interstices, resulting in higher apparent contact angles on rough surfaces compared to smooth surfaces. The measured contact angles in this study are expected to fit the Cassie-Baxter model rather than the Wenzel model [12].

In Figure 4 the average energy density ($\bar{E}$) delivered to laser treated samples, together with roughness and contact angle are plotted. The plotted logarithmic trendlines has a R squared value which indicates both a strong correlation, and in Fig.4 (b) moderate-to-strong correlation between the variables.

Figure 4. Plotted data of contact angle, roughness and average energy density of CuBr laser delivered to **(a)** Al 2219 alloy; **(b)** Al 1050 alloy samples.

The initial roughness of aluminum 2219 alloy was R_a 0.318 µm, R_z 4.19 µm, and R_q 0.387 µm, and the contact angle was 68°. After laser processing with an average energy density of 6 J/mm² delivered on aluminum alloy 2219, the roughness increased to R_a 5.52 µm, R_z 44.51 µm, and R_q 6.88 µm, and the contact angle reached a maximum of 134° (Figure 4.a). By increasing the average energy density by 16.67 times up to 100 J/mm², the roughness R_a increased by 3.03 times, R_z increased by 2.30 times, and R_q increased by 2.95 times as well as this change affected the contact angle, which decreased 6.70 times up to 20°. The wettability relative to initial material surface properties decreased 1.97 times when an average energy density of 6 J/mm² was applied, resulting in a hydrophobic surface. Conversely, an increase in wettability by 3.40 times was achieved when an average energy density of 100 J/mm² was applied, resulting in a hydrophilic surface.

The initial surface roughness of aluminum 1050 alloy was measured as R_a 0.156 µm, R_z 3.97 µm, and R_q 0.201 µm, and the contact angle was 73°. After laser processing with an average energy density of 0.88 J/mm² the roughness increased to R_a 2.04 µm, R_z 24.094 µm, and R_q 2.437 µm. As a result, the contact angle also increased to a maximum of 145° (Figure 4.b). Further increasing the average energy density by 181.81 times to 160 J/mm² caused a significant increase in roughness, with R_a increasing by 11.55 times, R_z increasing by 5.74 times, and R_q increasing by 11.48 times. This change also affected the contact angle, which decreased by 20.74 times, reaching a value of only 7°. As a consequence of laser processing, the surface wettability was altered relative to non-treated surface. Specifically, when an average energy density of 0.88 J/mm² was applied, the wettability decreased by 1.99 times, resulting in a hydrophobic surface. In contrast, increasing the average energy density to 160 J/mm² the wettability by 10.43 times also increases, resulting in a hydrophilic surface.

Figure 6 shows that the 3D morphology obtained by laser scanning microscopy provides a reliable representation of the correlation between surface irregularities and wetting properties. In the sample with CA 130° (Figure 5.d), the surface roughness creates micro-pockets in which air becomes caught, resulting in a high contact angle of the water droplet with roughness R_a 5,91 µm R_z 45,03 µm R_q 7,39 µm. Moreover, a decrease in the CA between the water droplet and the sample is accompanied by an increase of number of the micro-channels, which are interconnected and allows air to escape laterally during droplet-surface contact, thereby accelerates wettability to droplet to <10° where the trend for super hydrophilicity is observable (Figure 5.a) with roughness R_a 11.86 µm R_z 94.43 µm R_q 15.29 µm.
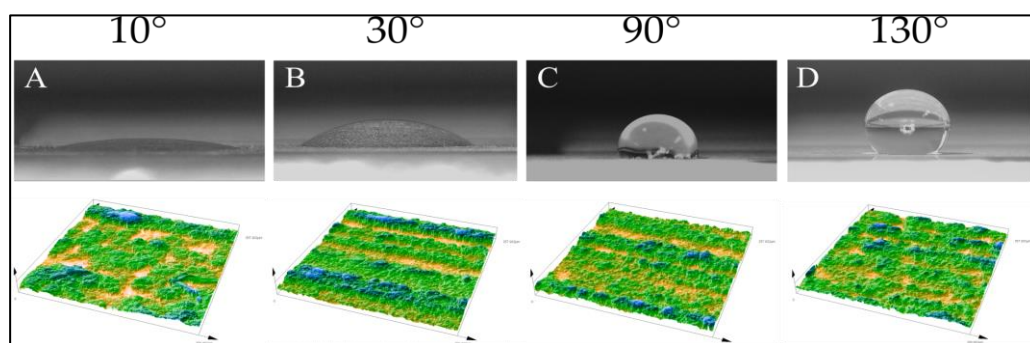
Figure 5. Droplets during the measurements of CA and a laser treated sample 3D surface morphologies of 2219 Al alloy.

Figure 6 data shows that for the laser treated specimen with CA 140° (Figure 6.d), the roughness of the surface creates small pockets where air gets trapped, leading to a high contact angle of the water droplet. The roughness values for this surface are R_a 1.90 μm, R_z 23.047 μm, and R_q 2.41 μm. Should be noted, that a decrease in contact angle between the water droplet and the sample is accompanied by an increase in the number of micro-channels that interconnect and allow air to escape laterally during droplet-surface contact, thus accelerating the wettability of the droplet. This results in a trend towards super hydrophilicity, observable also in Figure 5.a. Therefore specimen shown in Figure 6.a has roughness values of R_a 4.77 μm, R_z 44.35 μm, and R_q 6.07 μm.
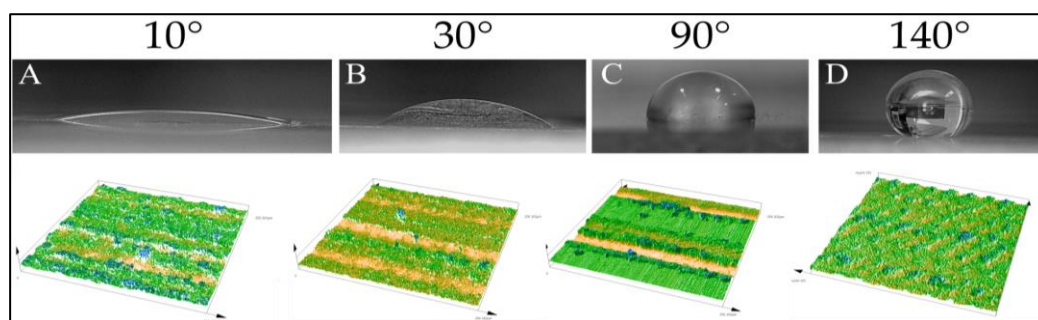
Figure 6. Droplets during the measurements of CA and a laser treated sample 3D surface morphologies of 1050 Al alloy.

In Figure 7 the pulse overlap (K_{ov}) is plotted together with roughness and CA. For Figure 7.a and Figure 7.b the trendlines were exponential with R squared value indicating strong correlation for Al 2219 and moderate correlation for Al 1050 alloys.

(**a**)

(**b**)
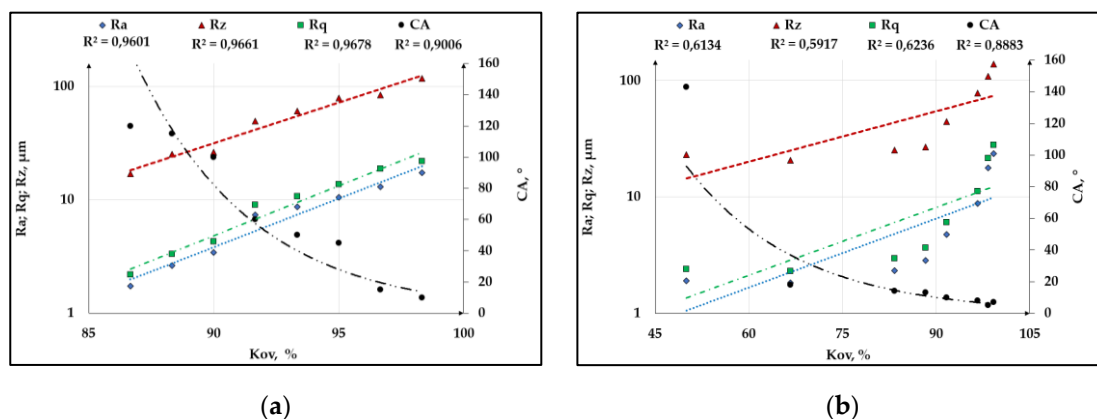
Figure 7. Plotted data of contact angle, roughness and pulse density of CuBr laser processing at 8 W average power (**a**) Al 2219 alloy; (**b**) Al 1050 alloy samples.

After laser processing with pulse overlap of 98% on aluminum alloy 2219, the roughness increased to Ra 11.86 μm, Rz 94.43 μm, and Rq 15.29 μm, and the contact angle reached an CA 10° (Figure 8.a).

By reducing pulse overlap 1.05 times till 93%, the roughness Ra reduced by 2.14 times, Rz reduced by 2.12 times, and Rq reduced by 2.22 times as well as this change affected the contact angle, which increased 13.40 times up to CA 134° (Figure 8.a). The wettability relative to initial material surface properties decreased 1.97 times when a pulse overlap of 93% was applied, resulting in a hydrophobic surface. Conversely, an increase in wettability by 6.8 times was achieved when a pulse overlap 98% was applied, resulting in a hydrophilic surface with CA 10°. Adjusting the pulse overlap during laser processing of aluminum alloy 2219 can significantly alter surface roughness and wettability, with a 93% pulse overlap resulting in decreased roughness and hydrophobicity, and a 98% pulse overlap resulting in increased wettability and hydrophilicity.

After subjecting aluminum alloy 1050 to laser processing with a pulse overlap of 99%, the surface roughness increased to Ra 23,564 μm, Rz 138,299 μm, and Rq 27,965 μm, and the contact angle was CA 7°. When the pulse overlap reduced 1.22 times to 83%, the surface roughness reduces by 11.55 times for Ra, 5.74 times for Rz, and 11.48 times for Rq. This change also has an impact on the contact angle, which increased 20.7 times to CA 145°, and the surface became hydrophobic with a decrease in wettability by 1.99 times relative to the initial material surface wetting. On the other hand, by applying a pulse overlap of 99%, the surface became hydrophilic, and the wettability increased by 10.42 times relatively to non-treated sample. Modifying the pulse overlap during laser processing of aluminum alloy 1050 can lead to significant changes in surface roughness and wettability, with a decrease in pulse overlap resulting in decreased roughness and increased hydrophobicity, and an increase in pulse overlap resulting in increased wettability and hydrophilicity.

The changes that occur during laser processing depend on the material physical properties, chemical composition and in surface properties. The same laser processing parameters utilized on two materials from different groups results in different properties occurred on the surface. Where the main factor is related in physical process of such technologies.

4. Conclusion

Within this research study, it has been determined that laser processing of materials close by chemical composition shows difference in change of roughness and wetting properties on the surface, thus the following conclusions could be made out of this study e.g. critical factors for change of roughness and wetting on the surface of treated materials are:

- Laser pulse overlap (K_{ov}), by increasing the overlap till 98-99% roughness increases gradually and this alters the transition to a hydrophilic surface CA 7°-10°. Main factor for wetting change is interconnected micro-chanels formation on the surface via laser processing.
- Reducing the overlap (K_{ov}) till 83-93% reduces the roughness, thus decreases the wettability and surface obtains hydrophobic properties 130°-145°. Main factor for wetting change is micro air pockets formation on the surface via laser processing.
- Increasing the average energy density ($\bar{E}$) delivered to the material 100 – 160 J/mm² results in roughness increment, thus altering the transition to a hydrophilic surface CA 7°-10°.
- Decreasing the average energy density ($\bar{E}$) delivered to the material 0.88 – 6 J/mm² results in roughness decrease and surface obtains hydrophobic properties 130°-145°.

References

1. Miroslaw Jonasz; Georges R. Fournier. Chapter 1 - Basic principles of the interaction of light with matter, Editor(s): Miroslaw Jonasz, Georges R. Fournier, Light Scattering by Particles in Water, Academic Press, 2007, Pages 1-32, ISBN 9780123887511, https://doi.org/10.1016/B978-012388751-1/50001-6.
2. Bloembergen, N. Laser-material interactions; fundamentals and applications. AIP Conference Proceedings. 1993 https://doi:10.1063/1.44887.
3. P. Pou-Álvarez, A. Riveiro, X.R. Nóvoa, M. Fernández-Arias, J. del Val, R. Comesaña, M. Boutinguiza, F. Lusquiños, J. Pou, Nanosecond, picosecond and femtosecond laser surface treatment of magnesium alloy: role of pulse length, Surface and Coatings Technology, Volume 427, 2021, 127802, ISSN 0257-8972, https://doi.org/10.1016/j.surfcoat.2021.127802.
4. Liang Zhang, Ning Zhao, Jian Xu, Fabrication and application of superhydrophilic surfaces: a review, Journal of Adhesion Science and Technology, 2014, pp. 769-790, https://doi.org/10.1080/01694243.2012.697714.
5. Balchev, Ivaylo & Minkovski, Nikolay & Dimitrov, Krassimir & Atanasov, A. & Stefanov, Plamen. (2015). CuBr laser ablation of titanium surface. Proceedings of SPIE - The International Society for Optical Engineering. https://doi.org/9447. 10.1117/12.2178086.
6. I.K. Kostadinov, K.A. Temelkov, D.N. Astadjov, S.I. Slaveeva, G.P. Yankov, N.V. Sabotinov, High-power copper bromide vapor laser, Optics Communications, Volume 501, 2021, 127363, ISSN 0030-4018, https://doi.org/10.1016/j.optcom.2021.127363.
7. Ahmed Olanrewaju Ijaola, Emmanuel Anuoluwa Bamidele, Cletus John Akisin, Idris Temitope Bello, Abiola Tunde Oyatobo, Abdullah Abdulkareem, Peter Kayode Farayibi, Eylem Asmatulu,Wettability Transition for Laser Textured Surfaces: A Comprehensive Review,Surfaces and Interfaces,Volume 21, 2020, 100802,ISSN 2468-0230, https://doi.org/10.1016/j.surfin.2020.100802.
8. M. M. Quazi, M. A. Fazal, A. S. M. A. Haseeb, Farazila Yusof, H. H. Masjuki & A. Arslan (2016) Laser-based Surface Modifications of Aluminum and its Alloys, Critical Reviews in Solid State and Materials Sciences, 41:2, 106-131, https://doi.org/10.1080/10408436.2015.1076716.
9. D.V. Zaitsev, K.A. Batishcheva, G.V. Kuznetsov, E.G. Orlova, Prediction of water droplet behavior on aluminum alloy surfaces modified by nanosecond laser pulses, Surface and Coatings Technology, Volume 399, 2020, 126206, ISSN 0257-8972, https://doi.org/10.1016/j.surfcoat.2020.126206.
10. Maxym V. Rukosuyev, Jason Lee, Seong Jin Cho, Geunbae Lim, Martin B.G. Jun, One-step fabrication of superhydrophobic hierarchical structures by femtosecond laser ablation, Applied Surface Science,Volume 313, 2014, Pages 411-417, ISSN 0169-4332, https://doi.org/10.1016/j.apsusc.2014.05.224.
11. L. Ruiz de Lara, R. Jagdheesh, J.L. Ocaña,Corrosion resistance of laser patterned ultrahydrophobic aluminium surface,Materials Letters,Volume 184, 2016, Pages 100-103,ISSN 0167-577X, https://doi.org/10.1016/j.matlet.2016.08.022.
12. Rafieazad, M., Jaffer, J., Cui, C., Duan, X. and Nasiri, A., 2018. Nanosecond Laser Fabrication of Hydrophobic Stainless-Steel Surfaces: The Impact on Microstructure and Corrosion Resistance. Materials, 11(9), p.1577. https://doi.org/10.3390/ma11091577.
13. Zhenhui Chen, Yue Lin, Qun Qian, Penghao Su, Yi Ding, Phan Dinh Tuan, Lisu Chen, Daolun Feng, Picosecond laser treated aluminium surface for photothermal seawater desalination, Desalination,Volume 528, 2022, 115561, ISSN 0011-9164, https://doi.org/10.1016/j.desal.2022.115561.
14. Atanasov, A. & Lengerov, Angel. (2021). INCREASING THE EFFECIENCY OF LASER MARKING OF ALUMINUM ALLOYS BY DOUBLE WRITING OF THE SYMBOLS. ENVIRONMENT. TECHNOLOGIES. RESOURCES. Proceedings of the International Scientific and Practical Conference. 3. 20-24. https://doi.org/10.17770/etr2021vol3.6550.